BRUKER

Tissue Clearing

A Short Techniques Review

Table of Contents

    WildDISCO
    SHANEL
    vDISCO
    FDISCO
    BALANCE
    EyeCi
    PEGASOS
    ECi
    uDISCO
    iDISCO+
    iDISCO
    3DISCO
    DBE
    Murray's Clear / BABB

    Fast 3D Clear
    DEEP-clear
    MACS
    OPTIclear
    RTF
    Ce3D
    FRUIT
    ClearSee
    CUBIC-Family
    SeeDB
    ClearT / ClearT2
    Scale Family

Cover

Cleared mouse embryo labeled with methylene blue (cyan) and showing autofluorescence (magenta). Image composed of 12 tiles and 920 planes, all processed and stitched with LuxBundle. Image courtesy of Montserrat Coll Lladó, European Molecular Biology Laboratory, Barcelona, Spain.

Introduction

Tissue-clearing techniques let researchers visualize three-dimensional (3D), large tissue structures by modifying the optical properties of opaque samples, rendering them transparent and accessible for light microscopy. Tissue-clearing techniques have become a valuable tool for the 3D analysis of the microstructure of biological tissues in neuroscience, connectomics, oncology, developmental biology, and organoid research.

High-resolution volumetric imaging of biological tissue has emerged as a crucial tool in cutting-edge biological research. Light-Sheet Fluorescence Microscopy (LSFM) leverages the optical advantages of cleared samples to enable fast, confocal-like optical sectioning and high-quality 3D imaging of cleared samples without the need for physical sectioning or destruction of the sample. LSFM allows rapid imaging of intact samples, from whole organs to entire organisms, while preserving the native 3D structure. LSFM has been adapted to image large, optically cleared (ex vivo) samples by implementing long working distance objectives, creative sample mounting, and larger imaging chambers.[1]

Light-Matter Interaction

The different refractive indexes (RI) of the major components of biological tissue, i.e., water, lipids, and proteins, result in light scattering when light passes through the tissue. The thicker the tissue is, the more prominent this effect becomes. Most biological samples are opaque in their native state due to light absorption and scattering. For these reasons, scientists have traditionally prepared samples into thin sections to visualize them with light microscopes. Tissue clearing modifies the optical properties of typically opaque samples to render them transparent while keeping their structure generally intact.[2] After clearing, light can travel through a sample unrestricted from absorption and scattering, ideal for high-resolution microscopic imaging deep within the specimen. There are numerous different clearing techniques, but all of them have one thing in common—they render biological samples optically transparent. The combination of tissue clearing with light-sheet microscopy is an ideal solution for addressing new questions in many fields of biology.
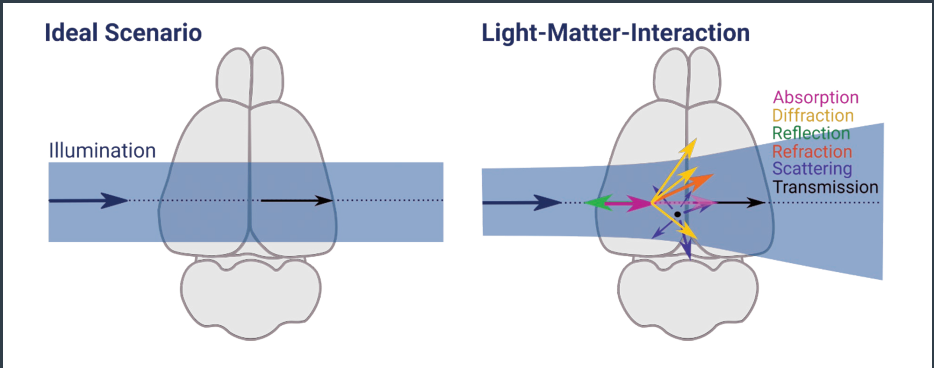
Ideal Scenario

Illumination

Light-Matter-Interaction

Absorption
Diffraction
Reflection
Refraction
Scattering
Transmission

FIGURE 1.
In an ideal scenario, light would penetrate 100% of a sample, but light-matter interaction, including absorption, diffraction, reflection, refraction, scattering, and transmission interfere with light transmission.

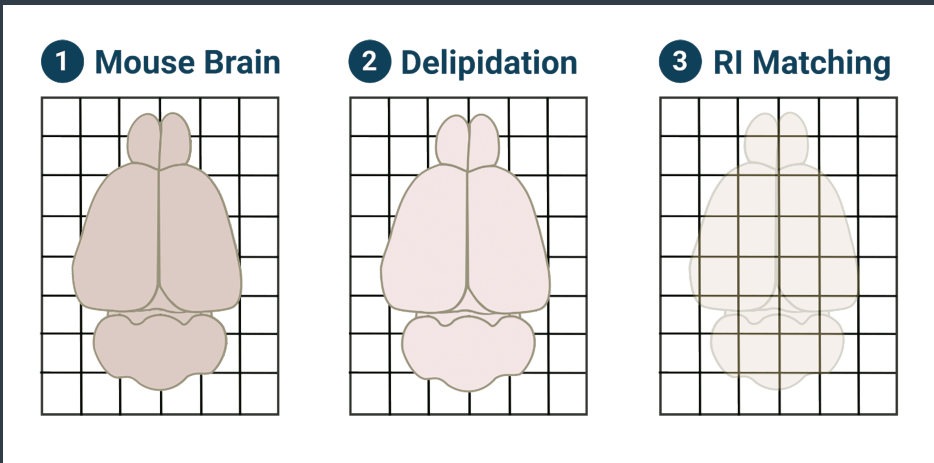**1 Mouse Brain**   **2 Delipidation**   **3 RI Matching**

FIGURE 2.
Tissue clearing modifies the optical properties of opaque samples, rendering them transparent and accessible for light microscopy. It increases light transmission through samples and allows the visualization of structures deep within tissues. It typically involves two steps: delipidation and RI matching.

Clearing Principles and Techniques

Method Overview for Tissue Clearing
Various tissue-clearing methods exist, each tailored to specific requirements and characteristics of the tissue and sample. There are a number of important considerations when choosing a protocol, including:

- Type of sample,

- Size of sample,

- Whether there is endogenous fluorescence to preserve,

- Compatibility with antibody labeling or nucleic acid hybridization,

- Ease-of-use,

- Speed, and

- Cost.

Preservation of Sample Size

Some protocols shrink tissue, while others cause tissue to expand, which may have advantageous or detrimental effects depending on the nature and purpose of the experiment. For example, scientists have used solvent-based methods to shrink and image entire mice,[3] or have taken advantage of tissue expansion to resolve structures smaller than the typical resolution limit of light microscopy.[4] On the other hand, tissue shrinkage may also reduce effective resolution, or tissue expansion may result in the sample size exceeding the working distance of your objective or the capacity of your sample chamber. Before starting your experiment, it is important to consider the protocol's effect on tissue size and how this may affect your results.
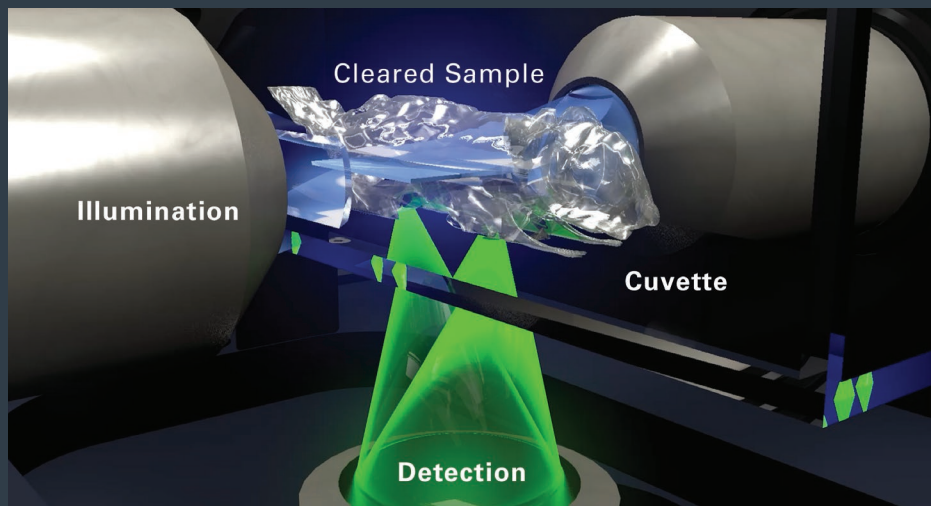
FIGURE 3.
Rendering of sample cuvette in the LCS SPIM with a cleared mouse sample
(illumination path: blue; detection path: green).

Types of Tissue Clearing

Approaches to tissue clearing vary based on experimental needs and samle types. Broadly speaking, there are four classes of clearing methods:

1. Hydrophobic Clearing Methods,

2. Hydrophilic Clearing Methods,

3. Hydrogel-Based Clearing Methods, and

4. Hyperhydration Clearing Methods, a.k.a. Expansion Microscopy.

Clearing protocols in each of these categories share characteristics that determine their suitability for particular applications. For example, solvent-based hydrophobic clearing methods dehydrate and shrink the sample, tend to have a high RI, and have short clearing times. They are effective in tissue with high lipid content but require immunofluorescence labeling methods.[5]

Water-based hydrophilic clearing methods work best for small samples, have limited clearing capacity, take a long time to clear, and work with both immunofluorescence and genetically encoded fluorophores.[6]

Hydrogel-based clearing methods entail a long and somewhat complex protocol but have a high clearing capacity due to efficient delipidation. They work well with immunofluorescence and genetically encoded fluorophores, and result in expanded tissues.[7]

Hyperhydration methods, also known as expansion microscopy,[8] are compatible with high-aperture (NA) water-immersion objectives and can achieve potentially higher resolution due to the expanded—and therein spatially better separated—structures. One disadvantage of expansion is that the signal intensity decreases due to lower label density.
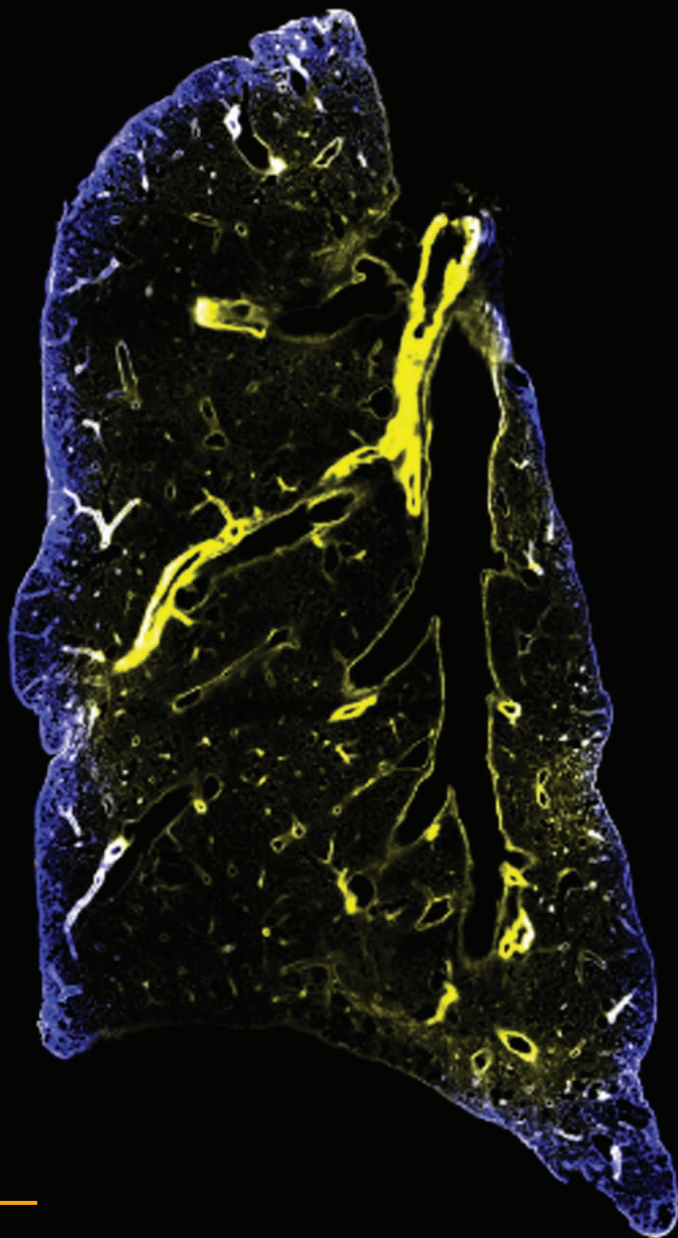
FIGURE 4.
Light-sheet images of a lung (single slice). Samples courtesy of Ayelen Melina, Santamans Recchini, and Gaudalupe Sabio Buzo, Stress Kinases in Diabetes, Cancer and Cardiovascular Disease Laboratory and Unit of Microscopy and Dynamic Imaging, Centro Nacional de Investigaciones Cardiovasculares Carlos III (CNIC), Madrid, Spain.

A good understanding of the available protocols can guide decision-making processes as individual methods have different strengths and weaknesses. Several excellent reviews in the literature provide an overview of tissue-clearing techniques, how they vary, and which may be suitable for particular applications.[2,9] Other publications offer a comparison of different techniques,[10-12] or considerations for neuroscience applications.[13] Lastly, decision trees are a useful tool for scientists while deciding on the right protocol to use for their specific application.[14,15]

Hydrophobic Clearing Methods

Hydrophobic clearing methods typically use an alcohol for dehydration, which leads to tissue shrinkage. This is followed by a step with solvents for delipidation and a clearing solution with an RI of approximately 1.56. These methods are typically low-cost and do not require specialized equipment.

Dehydration and delipidation shrink tissue, and the reagents of choice will affect the degree of tissue shrinkage. Some protocols take advantage of this effect to facilitate imaging of larger samples. Hydrophobic clearing solutions tend to be pure solutions, such as dibenzyl ether (DBE) or ethyl cinnamate (ECi), or miscible solutions, such as benzyl alcohol/benzyl benzoate (BABB). One advantage of this is that the imaging media rarely shows turgidity, which would substantially degrade image quality. DBE and BABB are most typically used due to their effectiveness, however, in many cases, ECi, a food-safe alternative to DBE and BABB, can be used instead.

WildDISCO
Immunolabeling of Wildtype Mice and DISCO Clearing
This method uses deep labeling of structures on centimeter scales with standard Immunoglobulin G (IgG) antibodies by enhanced cholesterol extraction before DISCO clearing. Heptakis(2,6-di-O-methyl)-β-cyclodextrin (CD5) was identified as a potent extractor of cholesterol, which is poorly removed by other solvent approaches. The addition of CD5 to the permeabilization buffer substantially increased the penetration of antibodies into centimeter-thick tissues. This approach is promising for labeling a wide variety of targets with commercially available antibodies, and over thirty have been validated by Mai et. al.[16]
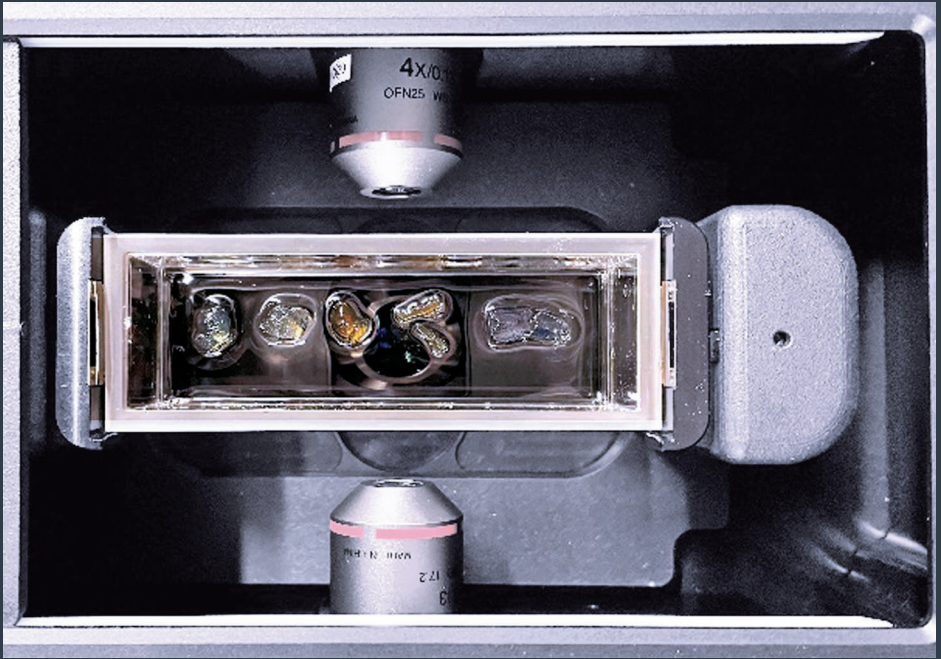
FIGURE 5.
Photograph of cleared mouse lung, heart, bone, and mouse head in the large LCS SPIM cuvette. Samples courtesy of Montserrat Coll Lladó, MIF, EMBL Barcelona, Spain.

Organic Solvent-Based Tissue Clearing

1 Mouse Brain 2 Immunostaining 3 Dehydration 4 Delipidation 5 RI Matching

Optional Tissue shrinkage

FIGURE 6.
Organic solvent-based tissue clearing follows a process that typically includes tissue fixation, optional immunostaining, dehydration, delipidation, and RI matching.

SHANEL

Small-Micelle-Mediated Human Organ Efficient Clearing and Labeling
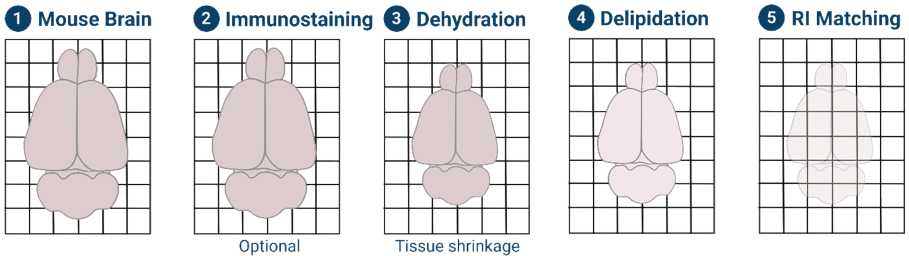This clearing method overcomes the challenges associated with fixed human tissue, such as light absorption and poor antibody diffusion.[17,18] This approach was developed to clear and image large volumes of human brain tissue, and an entire human brain has been cleared with this method. Unique features of this protocol include an initial decolorization step to remove residual blood, denaturation of the extracellular matrix with guanidine hydrochloride, and incorporation of (3-((3-cholamidopropyl) dimethylammonium)-1-propane sulfonate) (CHAPS) detergent for enhanced permeabilization. A disadvantage to this method is the bleaching of endogenous fluorescence.

vDISCO

Nanobody(VHH)-Boosted 3D Imaging of Solvent-Cleared Organs
As the immunolabeling of thick tissues is challenging, this was the first demonstration of the use of nanobodies for enhanced penetration compared to traditional IgG antibody staining.[19,20] To achieve this, the animals were perfused with a solution containing nanobodies, which are substantially smaller in molecular weight and size than IgGs, allowing deeper tissue penetration. Tissues were then subsequently cleared with a 3DISCO protocol. Nanobody perfusion produced greater penetration into deeper tissues and increased signal-to-noise ratios in areas otherwise challenging to immunolabel. The disadvantage of nanobody labeling is the lack of wide availability for specific targets compared to IgG antibodies.

FDISCO

DISCO with Superior Fluorescence-Preserving Capability
A modified 3DISCO protocol makes two key changes to the original protocol: the tetrahydrofuran (THF) solution is pH-adjusted to be more alkaline, and the incubations are done at 4 °C instead of room temperature.[21] The more alkaline conditions and cooler temperatures reduce the quenching of endogenous signal compared to uDISCO, leading ultimately to a better signal. One disadvantage to this method is that pH buffering the solutions in this protocol may be technically challenging.

BALANCE
Bleaching-Augmented Solvent-Based Non-Toxic Clearing
The Ethyl Cinnamate (ECi)-based clearing protocol is used to image mouse hearts.[22] Specific to this protocol are the low toxicity of the used reagents and the small number of chemicals required, so they are safe and cheap to use. In addition, this protocol effectively evens out differences in autofluorescence characteristics of heart tissue. While validated in the heart, this protocol has not been tested in other tissue types in the mentioned publication.

EyeCi
This is a combination of iDISCO and ECi protocols used for immunolabeling and clearing.[23] The EyeCi protocol is used on whole eyes of mice, as it is adapted for bleaching the melanin in the pigmented epithelium of the retina. One major advantage is the ability to process eye tissue without removing the cornea or lens. A drawback to this method is that the retina detaches, precluding imaging of intact opsins.

PEGASOS
Polyethylene Glycol-Associated Solvent System
Based on polyethylene glycol and ascorbate, this method has been proven to clear hard tissue, such as bones and teeth.[24] Thus, it has been applied for whole-body adult mouse clearing. The main PEGASOS steps include fixation, decalcification (hard tissue only), decolorization, delipidation, dehydration, and clearing. In short, the PEGASOS method efficiently clears all types of tissues except the pigmented retina. One major drawback of this method is that the clearing solution is a mixture, while most solvent-based methods use pure solutions. In practice, these mixtures can separate in the imaging chamber, which degrades image quality.

ECi
Ethyl Cinnamate-Based
This hydrophobic clearing method is known for its compatibility with immunostaining.[25] Introduced as a method to assess the total number of glomeruli in the kidney, it has become a welcomed alternative to DBE- and BABB-based clearing due to its food-safe properties. In many cases, it is possible to transfer samples in ECi after clearing them with most other hydrophobic clearing methods. One disadvantage of ethyl cinnamate is greater chromatic aberration than DBE or BABB.

uDISCO

Ultimate 3D Imaging of Solvent-Cleared Organs

This protocol is an improvement over the 3DISCO method, as 3DISCO produces a greater degree of tissue shrinkage and significantly decreases the rate of endogenous fluorescence quenching.[3] uDISCO shrinks tissue by approximately 50 to 60% while preserving endogenous fluorescence for months. uDISCO replaces THF (containing an ether group that is prone to reactivity) with tert-butanol, a tertiary alcohol that is more stable. The original clearing solution was modified to use a diphenyl ether, BABB, and Vitamin E mixture to reduce reactivity with endogenous fluorophores. DBE (which contains benzylic C-H and C-O bonds that can form peroxides) was replaced with diphenyl ether, which is less prone to peroxidation and free-radical formation. This protocol was applied to clear and image an entire mouse body for the first time. The major advantage of such a significant degree of tissue shrinkage is that it increases the sample size that can be imaged. One important consideration is that tissue shrinkage reduces the effective magnification of the imaging system.

iDISCO+

Improved Immunolabeling-Enabled Three-Dimensional Imaging of Solvent-Cleared Organs

The iDISCO protocol was modified to overcome brain-region-specific differences in tissue shrinkage, enabling registration of mouse brain data to a brain atlas.[26] iDISCO+ protocol replaced THF, which produces anisotropic shrinkage of brain tissue. THF was replaced with mixtures of methanol and dichloromethane (DCM) for dehydration and delipidiation. Removing THF from the protocol maintained the proportions between cortical and subcortical structures after clearing mediated shrinkage. While widely used, it is important to note that this protocol does not label large tissues evenly. In many cases, staining effectiveness rapidly decreases within <1 mm. Results are often improved by cutting away excess tissue around the area of interest or cutting a larger sample into pieces to increase antibody penetration.
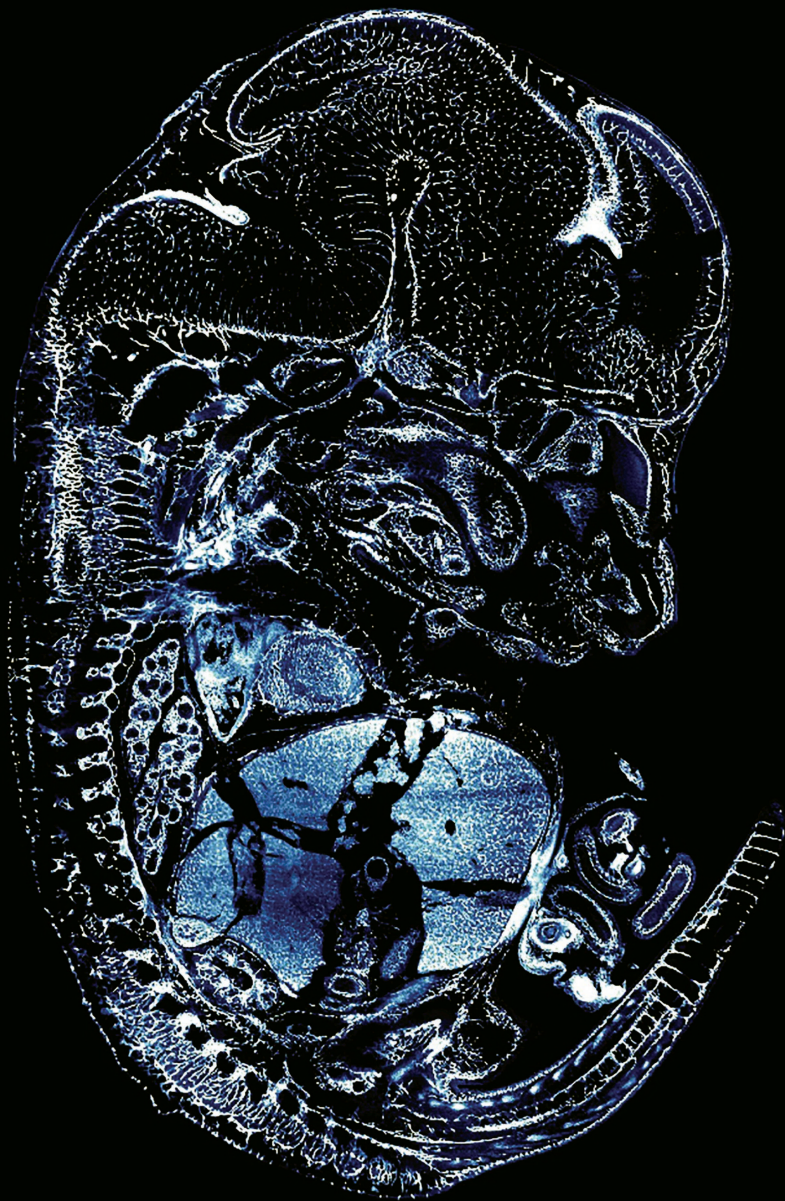
FIGURE 7.
Image acquired with the LCS SPIM of an iDISCO+ cleared E12.5 mouse embryo
labeled with anti-Flk1 (endothelial cell) antibody.
Sample courtesy of Sonja Nowotschin, Ying-Yi Kuo, and Kat Hadjantonakis,
MSKCC, New York, USA.

iDISCO

Immunolabeling-Enabled Three-Dimensional Imaging of Solvent-Cleared Organs
The iDISCO protocol described the first-time immunolabeling procedures that use widely available immunohistochemistry reagents for whole-organ labeling.[27] Samples are initially pre-treated with a methanol and hydrogen peroxide wash, a method to inactivate peroxidases and other enzymes that interfere with immunolabeling. Then, samples are permeabilized in detergents and blocked with serum to reduce non-specific antibody labeling. Once samples have been labeled, they are dehydrated and cleared using the 3DISCO protocol. Alexa Fluor-labeled signal is stable for months when stored in DBE as the final imaging solution. One drawback to this method is that it is incompatible with lipophilic dyes due to the solvents used for delipidation.

3DISCO

3D Imaging of Solvent Cleared Organs
This protocol improved upon the previous method[1] to clear myelinated structures in the central nervous system.[28] Dehydration was performed with THF, and the clearing was performed with DBE instead of BABB. This effectively cleared samples with high lipid content, such as mouse brain and spinal cord samples. This protocol has been adapted and serves as a basis for more complicated protocols that incorporate a labeling step. However, this protocol, as published, does not describe one. Endogenous fluorescence degrades after days.

DBE

Dibenzyl Ether
This study aimed to find a clearing reagent that better preserves green fluorescent protein (GFP) signal than BABB clearing.[29] Becker et al. figured DBE as an alternative that even provides slightly improved tissue transparency compared to BABB while significantly preserving the fluorescence intensity in GFP-expressing mouse brains. Using THF instead of ethanol for dehydration further increased fluorescence preservation in the tissue. While an improvement over BABB, endogenous fluorescence nonetheless rapidly diminishes over days.

Murray's Clear / BABB

Benzyl Alcohol and Benzyl Benzoate
This is a widely used hydrophobic clearing agent and one of the first demonstrations of tissue clearing paired with light-sheet imaging.[1] Ethanol and hexane are used for dehydration, with a 1:2 mixture of benzyl alcohol to benzyl benzoate for clearing. This protocol shrinks tissue, rapidly quenches endogenous fluorescence, and is ineffective in highly hydrophobic tissues, such as myelinated fiber tracts.
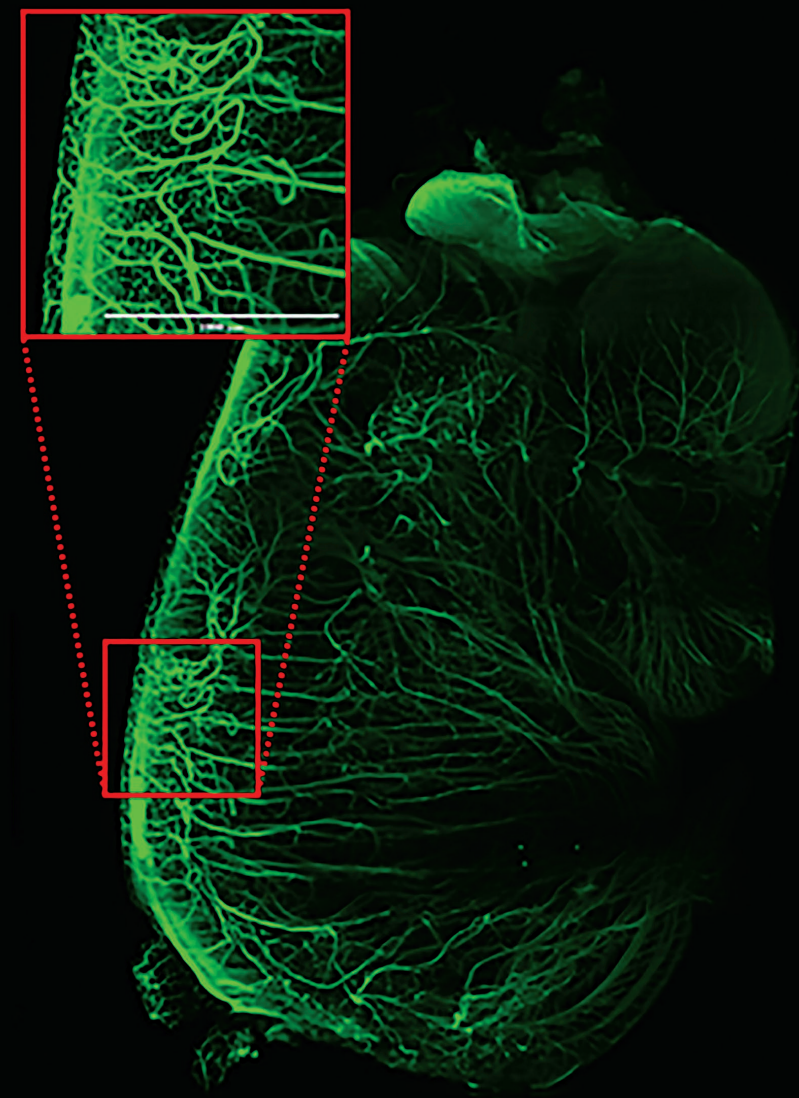
FIGURE 8.
Developing nerves in a whole mouse embryo. Sample cleared with DBE staining
TUJ1. Tiled image (3 x 4) acquisition. Scalebars: 1 mm. Imaged on the LCS SPIM.
Sample courtesy of James Muller, MSKCC, New York, USA.

Hydrophilic Clearing Methods

Hydrophilic methods are not expensive, easy to implement, and often retain compatibility with a wide range of fluorescent dyes and proteins, including lipid-targeting dyes. These methods typically use one of the following three approaches to reduce the scattering throughout a sample:

1. **Passive immersion** in a solution that is RI-matched to the tissue only gives good results for smaller samples. In simple immersion, the sample is placed in an aqueous solution containing a dissolved high-RI molecule. An RI of >1.45 needs to be reached to achieve adequate clearing of hydrated samples containing lipids.

2. **Removal of lipids followed by hydration** of the sample with the goal of lowering the RI of the remaining tissue components. This method aims to maintain an aqueous environment for fluorescent proteins and commonly reduces the overall RI to <1.4.

3. **Active or passive removal of lipids** followed by immersion in an RI-matched medium.[2]

Fast 3D Clear

Fast 3D Clear uses urea-enriched tetrahydrofuran (THF) and iohexol (Histodenz).[30] THF is utilized for tissue delipidation, while Histodenz facilitates tissue clearing. This has the advantage that the sample can be imaged under immersion oil in light-sheet imaging systems. It takes three days to render adult and embryonic mouse tissues transparent. Importantly, anatomical integrity and a wide range of transgenic and dye fluorophores are preserved during the clearing process. The clearing process with Fast 3D Clear is fully reversible, making it compatible with tissue sectioning and immunohistochemistry.

DEEP-clear

Depigmentation-Plus-Clearing
This method combines depigmentation with tissue clearing.[31] It was originally showcased on five different species representing four distinct animal clades (annelids, molluscs, bony fishes, and tetrapods). DEEP-Clear efficiently removes naturally occurring pigments (such as pterins, ommochromes, heme, carotenoids, and melanin). It is compatible with immunohistochemical (IHC) analysis in samples fixed with either paraformaldehyde (PFA) or Bouin's fixative.

Aqueous Hyper-Hydrating Tissue Clearing

1 **Mouse Brain** 2 **Immunostaining** 3 **Depigmentation** 4 **Delipidation** 5 **RI Matching**
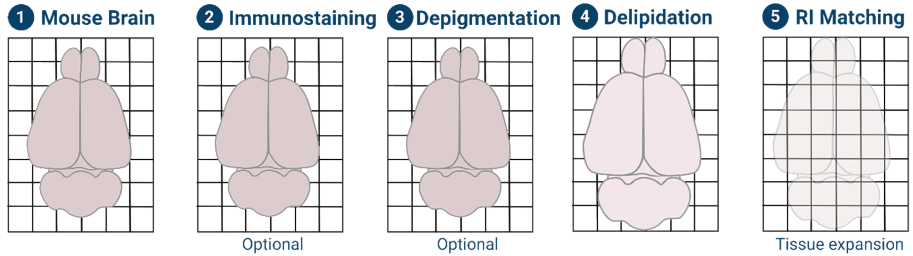
Optional Optional Tissue expansion

FIGURE 9.
Principle of aqueous hyper-hydrating tissue clearing, which involves fixation, optional immunostaining, optional depigmentation, delipidation, and RI matching.

MACS

MXDA-Based Aqueous Clearing System
This was the first clearing method that introduced m-xylylene diamine (MXDA) as a clearing agent to replace urea.[32] It was applied to investigate diverse mouse organs' morphological, physiological, and pathological properties.

OPTIclear

Optical Properties-Adjusting Tissue-Clearing Agent
OPTIclear overcomes the differences between rodent and primate brains, including variations in gross size, physiochemical properties, and neuronal and myelin densities.[33] This agent is specifically designed for both fresh and archival human brain tissue and can even be applied to formalin-fixed, paraffin-embedded material. Its formulation comprises three principal components: 20% w/v N-methylglucamine, 25% w/v 2,2'-Thiodiethanol, and 32% w/v Iohexol. This method was first applied to tissue that was only a few mm thick. The resulting RI was around 1.47–1.48.

RTF

Rapid Clearing Method Based on Triethanolamine and Formamide
RTF is based on ClearT2 and is optimized for adult mouse brain blocks and mouse embryos.[34] It preserves the fluorescent signal of both endogenous fluorescent proteins and lipophilic dyes. The resulting RI was 1.44.

Ce3D

Ce3D was invented to enhance multicolor fluorescence imaging. It preserves cellular morphology and protein fluorescence and is robustly compatible with antibody-based immunolabeling.[35] This enhanced signal quality and capacity for extensive probe multiplexing permits quantitative analysis of distinct, highly intermixed cell populations in intact Ce3D-treated tissues via 3D histo-cytometry. Main components are N-methylacetamide, Histodenz with small portions of Thioglycerol and Triton-X. The final Ce3D medium has an RI of approximately 1.5.

FRUIT

This unique clearing method is known for its gentle treatment of delicate samples.[36] Based on SeeDB, it takes advantage of the synergistic effect of fructose and urea on clearing. Applied initially to clearing large-scale mammalian brains, it is compatible with yellow fluorescent protein and preserves the fluorescence of lipophilic tracers without damaging the cellular plasma membrane. The resulting RI was 1.48.

ClearSee

This clearing technique was developed for deep imaging of morphology and gene expression in plant tissues.[37] ClearSee is based on the Scale protocol and rapidly diminishes chlorophyll autofluorescence while maintaining fluorescent protein stability. Exercising the protocol is time-consuming, but by doing so, whole-organ and whole-plant imaging can be performed. ClearSee mainly consists of xylitol powder [final 10% (w/v)], sodium deoxycholate [final 15% (w/v)] and urea [final 25% (w/v)] mixed in water. The final imaging solution has to be adjusted to compensate for potential RI mismatch.

CUBIC-Family

Clear, Unobstructed Brain/Body Imaging Cocktails
Starting by modifying the Scale protocol and coming up with ScaleCUBIC-1 and ScaleCUBIC-2, a whole family of similar clearing protocols arose, adapting to specific aspects of the sample.[38,39] The novelty here was to actively screen forty chemicals toward their clearing efficiency on tissues, resulting in basic amino alcohols being best suited. Based on the first CUBIC protocol (CUBIC-1), the clearing efficiency and speed were enhanced in CUBIC-2. The protocols have been specifically adapted: CUBIC-L stands for lipophilic, and CUBIC-LH stands for lipophilic reagents, in addition to hydrophilic ones, and leads to enhanced tissue transparency and fluorescence preservation. It is particularly useful for lipid-rich tissues and organs. CUBIC-R improved the RI-matching, whereas CUBIC-X combines fluorescent-protein-compatible, whole-organ clearing and homogeneous eXpansion. CUBIC-R2 is an advanced variant (Refractive Index Matching and Reduced Tissue Shrinkage), combining RI matching with measures to minimize tissue shrinkage, enhancing imaging depth while maintaining tissue integrity. The resulting RI is 1.45.

SeeDB

See Deep Brain
This method was originally developed to facilitate comprehensive and quantitative analyses for understanding neuronal circuitry.[40] The major focus was to keep the fine morphology and the sample volume intact during the clearing procedure. SeeDB clears fixed brain samples in a few days without quenching many types of fluorescent dyes, including fluorescent proteins and lipophilic neuronal tracers. The clearing solution is a saturated solution of fructose (80.2% wt/wt) in water with 0.5% α-thioglycerol. The resulting RI is 1.48.

ClearT / ClearT2

ClearT or ClearT2, which are composed of formamide or formamide/polyethylene glycol, respectively, have been among the first clearing methods that did not use detergents or solvents.[41] Thus, preserved lipophilic dyes, fluorescent tracers, immunohistochemical labeling, and fluorescent-protein labeling can be used. Embryos, whole mounts, and thick brain sections can be cleared with minimal volume changes. The resulting RI is 1.44.

Scale Family

The Scale family includes methods like ScaleA2, ScaleU2, ScaleB4, and ScaleS.[42] All the Scale family methods completely preserve fluorescent signals in the clarified tissue. Whereas ScaleA2 causes the sample to expand noticeably (1.25x), ScaleU2 was designed to reduce the tissue expansion and fragility caused by the clearing procedure.

ScaleA2 started the Scale family using 4M urea, glycerol, and Triton X-100 as the main components.[42] The clearing process takes days to weeks, depending on the volume, and induces noticeable tissue expansion. Clearing a mouse brain, for example, takes around two weeks. This results in an RI of 1.38.

ScaleU2 significantly reduces tissue expansion compared to ScaleA2 by using a higher percentage of glycerol, but needs much longer incubation times to achieve clearing.[42] This results in an RI 1.38.

ScaleB4 significantly depletes background signals in the tissue and shows a faster clearing process.[42] 8M urea is used instead of 4M (see above ScaleA2), no glycerol, and Triton X-100. This results in an RI of 1.37.

ScaleS uses sorbitol to counteract the tissue expansion caused by urea.[43] Urea causes hydration (expands tissue), and sorbitol causes dehydration (shrinks tissue). By using the correct ratio, the two effects can be balanced, and the tissue volume is preserved. ScaleS is compatible with immunochemical labeling and was first applied to optically reconstruct aged and diseased brains in Alzheimer's disease models, including mapping of 3D networks of amyloid plaques, neurons, and microglia. This results in an RI of 1.44.

FIGURE 10.
Sample imaged
on the LCS
SPIM.
Courtesy of
Dr. Chenchen Pan,
DKFZ, Heidelberg,
Germany.
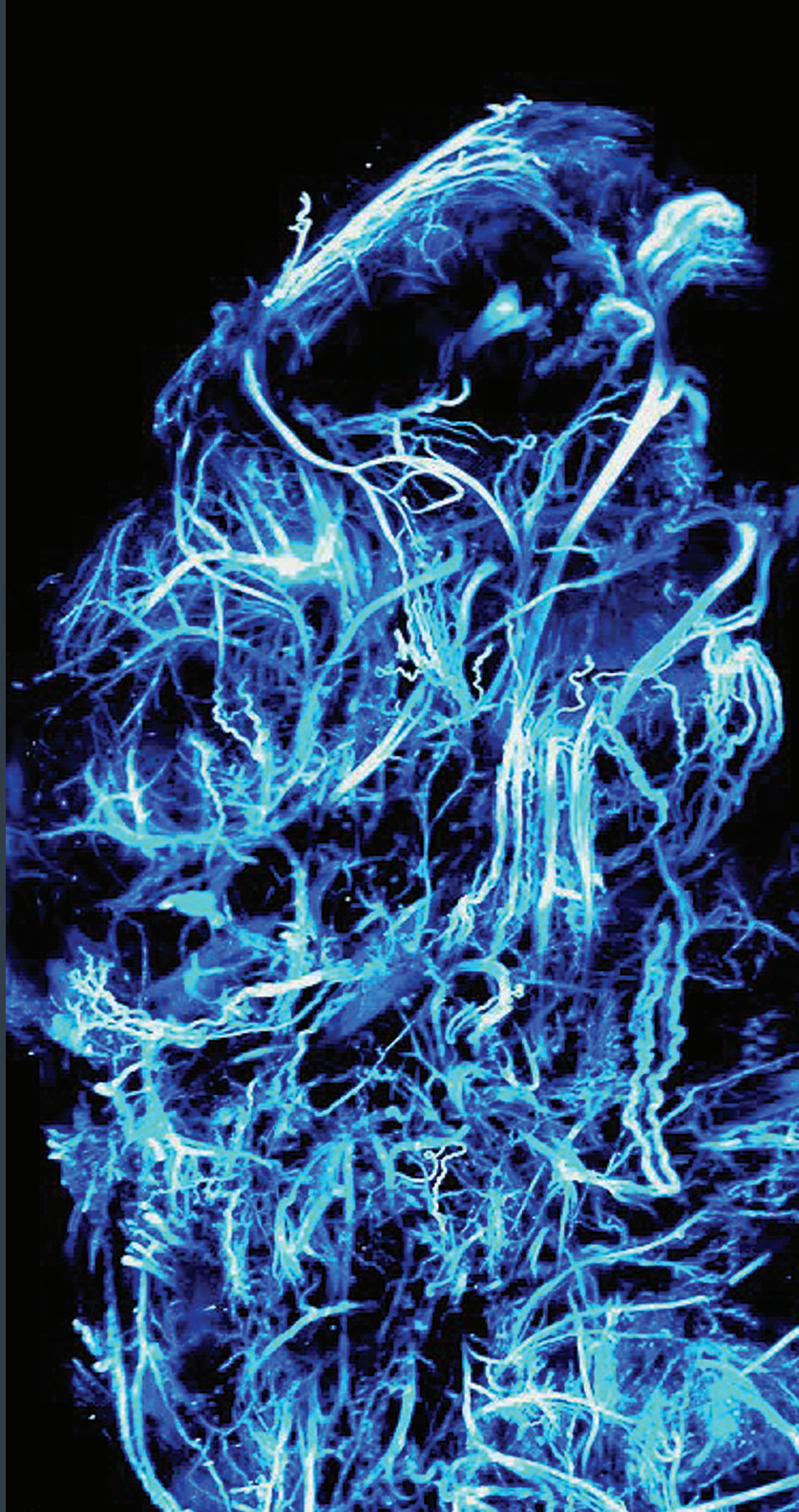
Hydrogel-Based Clearing Methods

Hydrogel-based methods involve crosslinking hydrogel and fixative molecules to tissue and often involve electrophoresis in detergent solutions for delipidiation. Some methods use electrophoresis to assist labeling. Thus, some of the protocol novelty lies in creating a hydrogel from the sample, with individual protocols varying depending on the material properties needed. RI-matching solutions are aqueous mixtures with high concentrations of solute to raise the RIs to approximately 1.45. Hydrogel methods can preserve endogenous fluorescence and a broad range of proteins and nucleic acids. Some protocols preserve original tissue dimensions, while others may expand and distort depending on the hydrogel characteristics. Disadvantages of these methods include the need for specialized equipment in many cases.

eFLASH
Electrophoretically Driven Fast Labeling Using Affinity Sweeping in Hydrogel
This protocol uses epoxide crosslinking (SHIELD, see below) as an initial fixation step, followed by electrophoretic labeling in a buffer that gradually increases antibody affinity. Antibody binding is initially low and gradually increases as the electrophoretic reaction progresses.[44] This allows for the even diffusion of antibodies into the tissue before they bind to their target antigens, giving uniform labeling in larger tissues. The advantage of this protocol is fast and controlled immunolabeling. However, this protocol requires specialized equipment that is capable of rotating a sample while performing electrophoresis. The resulting RI is 1.46.

SHIELD
Stabilization to Harsh Conditions via Intramolecular Epoxide Linkages to Prevent Degradation
The SHIELD protocol uses an epoxide backbone to fix tissue while preserving epitopes, protein conformation, and endogenous fluorescence.[45] The epoxide backbone provides an exceptionally rigid and stable network for preserving both crosslinking protein and nucleic acids during clearing. This protocol can be combined with SWITCH to preserve endogenous fluorescence while allowing for multiple rounds of clearing and multiplexed labeling. One important consideration is that labeling may need to be done via an active method, such as stochastic electrotransport. The resulting RI is 1.4, without tissue shrinkage and expansion.
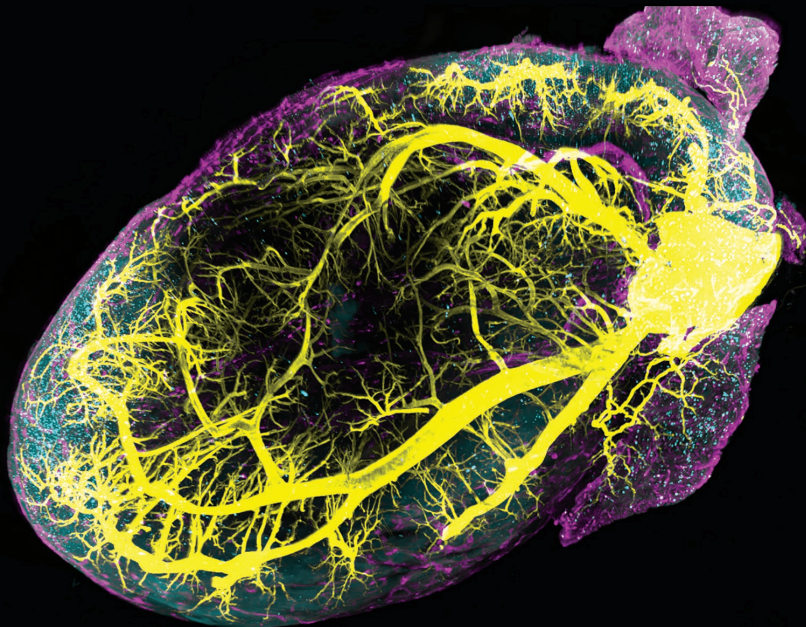
FIGURE 11.
Cleared mouse heart imaged with the LCS SPIM, with 488 nm showing tissue autofluorescence (cyan), 561 nm showing the microvasculature (yellow), and 642 nm showing the microvasculature (magenta). Samples courtesy of Luis Diago Domingo and Rui Benedito, Laboratory of Molecular Genetics of Angiogenesis, and the Microscopy and Dynamic Imaging Unit of the Carlos III National Center for Cardiovascular Research (CNIC) in Madrid, Spain.

Hydrogel Embedding Tissue Clearing

1 **Mouse Brain**   2 **Hydrogel Polymerization**   3 **Immunostaining**   4 **Delipidation**   5 **RI Matching**

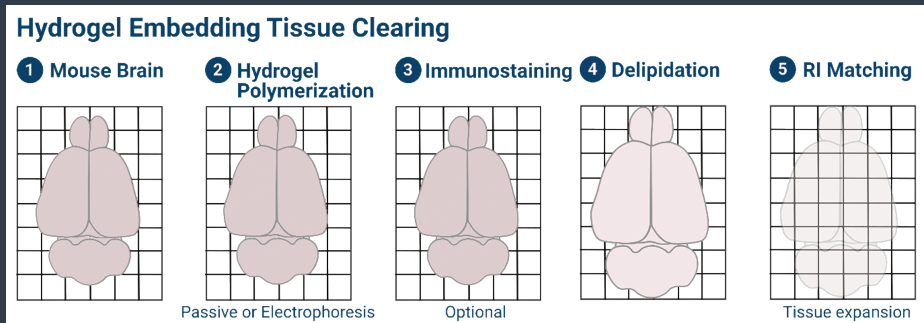Passive or Electrophoresis   Optional   Tissue expansion

FIGURE 12.
Principle of hydrogel embedding tissue clearing, which involves fixation, active or passive hydrogel polymerization, optional immunostaining, delipidation, and RI matching.

ACT-PRESTO

Active Clarity Technique-Pressure Related to Efficient and
Stable Transfer of Macromolecules into Organ
ACT-PRESTO made several improvements to the original CLARITY
protocol (see below).[46] The fixation and clearing procedure were
modified to a two-step procedure so that the hydrogel-tissue
network is less dense. This allowed for faster electrophoretic
clearing. This system was termed *active clarity technique* (ACT)
and could clear a mouse brain in less than one day. In addition,
the authors tried to overcome limited diffusion of antibodies into
brain tissue using pressure-related efficient and stable transfer of
macromolecules into organs (PRESTO). While pressure enhances
the diffusion of antibodies into tissue cleared with this method,
overall penetration is not very effective at millimeter scales, which
may impede the labeling of larger samples. One major difference
between ACT-PRESTO and the original CLARITY protocol is that
the lower-density hydrogel leads to a much greater degree of
tissue expansion, which may not be beneficial depending on the
application. The resulting RI is 1.43 to 1.48, with tissue expanding.

SWITCH

System-Wide Control of Interaction Time and Kinetics of Chemicals
The SWITCH protocol aimed to control the kinetics of chemical
reactions within the tissue to evenly distribute agents for fixation
and labeling within tissue before activating the reactions.[47] To do
this, the authors developed SWITCH-Off buffering solutions that
allowed diffusion without reaction and then activation with SWITCH-
On buffers once diffusion was complete. This overcomes the issue
that fixation and labeling occur on the surface of thick tissues before
permeating deeper inside, which typically results in uneven labeling.
The authors were able to use this method to create a rigid hydrogel
that would be resistant to the harsh conditions of multiple rounds
of clearing and labeling for highly multiplexed imaging. The authors
demonstrate that at least twenty rounds of imaging are possible
with this method. It is important to note that the on and off buffers
vary in pH and use high detergent concentrations, which may not
be compatible with all types of probes. The resulting RI is 1.47, with
tissue expanding.

PACT

Passive Clarity Technique

PARS

Perfusion-Assisted Agent Release in Situ

The reagents in this protocol improve upon the original CLARITY technique so that the delipidation is done passively and does not require electrophoresis.[48] The PACT reagents can be infused into the vasculature or intracranially, followed by perfusion-assisted agent release in situ - termed PARS. The advantages of this protocol are preservation of endogenous fluorescence, compatibility with antibody labeling, and nucleic acid hybridization. The disadvantage of the passive approach is that the sample size is limited without electrophoresis. The resulting RI is 1.38 – 1.48, with tissue expanding.

CLARITY

Clear Lipid-Exchanged Acrylamide-Hybridized Rigid Imaging /
Immunostaining / In situ-Hybridization-Compatible Tissue Hydrogel

This method was the first demonstration of tissue clearing by creating a tissue-hydrogel network and initiating delipidation with electrophoresis in a detergent solution.[7] This protocol infuses tissue with hydrogel monomers and formaldehyde to crosslink proteins. Then, the monomers are polymerized using heat in hypoxic conditions. Delipidiation is then performed using electrophoresis. Advantages of this method include preservation of endogenous fluorescence, compatibility with nucleic acid hybridization, and capability for multiple rounds of labeling. However, antibody penetration is relatively poor in practice, and tissue expansion occurs anisotropically. The resulting RI is 1.45, with tissue expanding.

Expansion Microscopy Methods

The resolving power of fluorescence microscope systems is limited due to the diffraction limit of approximately half the wavelength of light used for observation. This prevents imaging of many subcellular structures of interest smaller than several hundred nanometers. Expansion microscopy refers to a class of methods that enhance the resolution limit of an imaging system by increasing the dimensions of the sample of interest. The general principle involves infusing a sample of interest with a solution of monomers that can polymerize to form a hydrogel network with covalent bonds anchoring the target of interest. These polymers expand when immersed in water, which causes the linear dimensions of the sample to swell between approximately fourfold and twentyfold. The expanded and hydrated samples incorporate enough water to effectively clear samples and match the index of refraction to that of water. This enables the use of water-immersion diffraction-limited microscope systems at effective resolutions that approach super-resolution methods. Specifically, it can be used in combination with light-sheet microscopy to allow the acquisition of great depths.

Advantages of expansion methods include the ability to preserve endogenous fluorescence, greater epitope presentation in expanded samples, and the use of water as an imaging media, which is compatible with many commercially available imaging systems. Disadvantages include dimmer labeling signal due to greater separation of fluorophores and decreased sample rigidity, which can make mounting challenging. Many protocols are optimized for the retention of either protein or nucleic acids, but most do not preserve both. An important consideration is that increased sample sizes require the use of long working distance objectives and large sample chambers. All of the following protocols use water as immersion media for imaging with an RI of approximately 1.33.

Magnify
Magnify was developed as an easy-to-use protocol using widely available reagents that are compatible with a wide array of molecules.[49] Magnify provides greater than tenfold expansion and is compatible with typically challenging tissues, such as kidneys. This protocol combines the anchoring and gelation steps using methacrolein, which serves as both fixative and monomer for polymerization. Gel-embedded samples are then treated with high temperatures in a denaturant solution. Advantages include the ability to preserve and label proteins, nucleic acids, and lipids using the same protocol. The reported effective resolution is approximately 25 nm.

X10

Expansion Microscopy
The goal of this protocol was to develop an expansion method
that approaches the resolution of super-resolution systems but
does not need any specialized equipment or custom reagents to
perform.[50] Here, the authors achieve greater expansion in a single
step compared to previous reports, with a tenfold expansion in
each dimension and approximately 25 nm effective resolution.
The hydrogel components include N, N-dimethylacrylamide acid,
and sodium acrylate, with Acrylol-X anchoring proteins to the gel,
similar to the ProExM method. One disadvantage is that protease
digestion with this method does not preserve endogenous
fluorescent proteins.

iExM

Iterative Expansion Microscopy
This protocol modifies the original expansion microscopy protocol
(see below ExM-protocol) by adding a second polymerization
and expansion step.[51] After the sample is expanded initially by
approximately four-and-a-half fold, it is polymerized again, and the
original gel is digested. The second round of expansion further
increases magnification by approximately fourfold, giving an overall
approximately twentyfold increase in sample magnification. This
iterative protocol greatly increases the overall expansion factor
and enables imaging at approximately 25 nm effective resolution
with antibody labeling. The disadvantage of this method is the
resolution is limited by the size of antibodies and the twenty
fold expansion factor.

ProExM

Protein-Retention Expansion Microscopy
This protocol allows for imaging endogenous fluorescent proteins
and was the first to enable the use of commercial antibodies and
genetically encoded reporters.[52] The key difference compared to
the original ExM protocol is the use of acryloyl-X as an anchor to
bind endogenous proteins and antibodies to the hydrogel network.
Proteinase K was used for protease digestion as it effectively
cleaves proteins for uniform expansion while leaving fragments
large enough to preserve fluorescence. This has enabled greater
adoption of expansion microscopy as reagents are commercially
available. One important consideration mentioned is that overall
label brightness is decreased. Protease digestion reduces both
endogenous protein and secondary antibody fluorescence.
However, acryloyl-X retains signal across a variety of fluorophores
to varying degrees.

ExM

Expansion Microscopy

This report was the first demonstration of expansion microscopy.[4] Samples were permeabilized with sodium acrylate and acrylamide monomers, cross-linked with N-N'-methylenebisacrylamide, and polymerized with a free-radical initiator. Protease treatment mechanically dissociates the network, and when placed in water, the samples expand approximately four-and-a-half fold. Expanded samples were imaged with an effective resolution of approximately70 nm laterally and 200 nm axially. The disadvantage of this method is that protease treatment precludes traditional antibody labeling. Additionally, the specialized DNA oligonucleotides used in this publication for labelling are not commercially available.

Conclusion

Tissue clearing has become a vital part of optical imaging of biological tissues, organs, and entire animal models in their native, i.e., 3D volumetric, state. These clearing techniques modify the optical properties of originally opaque samples, rendering them transparent while keeping the physiological context intact. Transparency is the ideal prerequisite for high-resolution microscopic imaging deep within mesoscopic samples. As a result, the combination of tissue clearing with light-sheet microscopy is a perfect synergistic solution since light-sheet microscopy enables imaging deep in volumetric tissues as long as these regions are optically accessible, i.e., transparent samples.

The diversity of tissue-clearing methods, each tailored to specific requirements and characteristics of the tissue and sample, allows one to choose the most suitable approach for the experimental goals. Hydrophobic, hydrophilic, hydrogel-based, and hyperhydration clearing methods (expansion microscopy) each have their unique strengths and limitations. The choice of method depends on a number of factors, including the type and size of the sample, the presence of endogenous fluorescence, compatibility with antibody labeling or nucleic acid hybridization, ease of use, speed, and cost.

While some protocols cause tissue to shrink or expand, which can be advantageous or detrimental depending on the nature of the experiment, others preserve the original tissue dimensions. Some methods require specialized equipment, while others are easy to implement and often retain compatibility with a wide range of fluorescent dyes and proteins, including lipid-targeting dyes. The choice of method depends on specific research needs, sample characteristics, and available resources, so it is recommended to select the most suitable approach based on the experimental goals.

References

1. Dodt, H. U., U. Leischner, A. Schierloh, N. Jährling, C. P. Mauch, K. Deininger, J. M. Deussing, M. Eder, W. Zieglgänsberger, and K. Becker. 2007. "Ultramicroscopy: three-dimensional visualization of neuronal networks in the whole mouse brain." *Nat Methods* 4 (4): 331-6.
https://doi.org/10.1038/nmeth1036.
https://www.ncbi.nlm.nih.gov/pubmed/17384643.

2. Richardson, D. S., and J. W. Lichtman. 2015. "Clarifying Tissue Clearing." Cell 162 (2): 246-257.
https://doi.org/10.1016/j.cell.2015.06.067.
https://www.ncbi.nlm.nih.gov/pubmed/26186186.

3. Pan, C., R. Cai, F. P. Quacquarelli, A. Ghasemigharagoz, A. Lourbopoulos, P. Matryba, N. Plesnila, M. Dichgans, F. Hellal, and A. Ertürk. 2016. "Shrinkage-mediated imaging of entire organs and organisms using uDISCO." *Nat Methods* 13 (10): 859-67. https://doi.org/10.1038/nmeth.3964.
https://www.ncbi.nlm.nih.gov/pubmed/27548807.

4. Chen, F., P. W. Tillberg, and E. S. Boyden. 2015. "Optical imaging. Expansion microscopy." *Science* 347 (6221): 543-8.
https://doi.org/10.1126/science.1260088.
https://www.ncbi.nlm.nih.gov/pubmed/25592419.

5. Molbay, M., Z. I. Kolabas, M. I. Todorov, T. L. Ohn, and A. Ertürk. 2021. "A guidebook for DISCO tissue clearing." *Mol Syst Biol* 17 (3): e9807.
https://doi.org/10.15252/msb.20209807.
https://www.ncbi.nlm.nih.gov/pubmed/33769689.

6. Wang, Peixin, Dan Zhang, Shaocong Bai, Benzhang Tao, Shiqiang Li, Tao Wang, and Aijia Shang. "Feasibility of commonly used fluorescent dyes and viral tracers in aqueous and solvent-based tissue clearing." *Neuroscience Letters* 737 (2020): 135301. https://doi.org/10.1016/j.neulet.2020.135301. https://pubmed.ncbi.nlm.nih.gov/32784007/.

7. Chung, K., and K. Deisseroth. 2013. "CLARITY for mapping the nervous system." *Nat Methods* 10 (6): 508-13.
https://doi.org/10.1038/nmeth.2481.
https://www.ncbi.nlm.nih.gov/pubmed/23722210.

8. Zhuang, Y., and X. Shi. 2023. "Expansion microscopy: A chemical approach for super-resolution microscopy." *Curr Opin Struct Biol* 81: 102614. https://doi.org/10.1016/j.sbi.2023.102614. https://www.ncbi.nlm.nih.gov/pubmed/37253290.

9. Richardson, D. S., W. Guan, K. Matsumoto, C. Pan, K. Chung, A. Ertürk, H. R. Ueda, and J. W. Lichtman. 2021. "TISSUE CLEARING." *Nat Rev Methods Primers* 1 (1). https://doi.org/10.1038/s43586-021-00080-9. https://www.ncbi.nlm.nih.gov/pubmed/35128463.

10. Hongcheng, Mai, and Lu Dan. 2024. "Tissue clearing and its applications in human tissues: A review." *VIEW* 5, no. 2 (2024): 20230046.https://doi.org/10.1002/VIW.20230046. https://onlinelibrary.wiley.com/doi/10.1002/VIW.20230046.

11. Matryba, Paweł, Leszek Kaczmarek, and Jakub Gołab. 2019. "Advances in Ex Situ Tissue Optical Clearing." *Laser & Photonics Reviews*. https://doi.org/10.1002/lpor.201800292. https://onlinelibrary.wiley.com/doi/full/10.1002/lpor.201800292.

12. Yu, T., J. Zhu, D. Li, and D. Zhu. 2021. "Physical and chemical mechanisms of tissue optical clearing." *iScience* 24 (3): 102178. https://doi.org/10.1016/j.isci.2021.102178. https://www.ncbi.nlm.nih.gov/pubmed/33718830.

13. Ueda, H. R., A. Ertürk, K. Chung, V. Gradinaru, A. Chédotal, P. Tomancak, and P. J. Keller. 2020. "Tissue clearing and its applications in neuroscience." *Nat Rev Neurosci* 21 (2): 61-79. https://doi.org/10.1038/s41583-019-0250-1. https://www.ncbi.nlm.nih.gov/pubmed/31896771.

14. Muntifering, M., D. Castranova, G. A. Gibson, E. Meyer, M. Kofron, and A. M. Watson. 2018. "Clearing for Deep Tissue Imaging." *Curr Protoc Cytom* 86 (1): e38. https://doi.org/10.1002/cpcy.38. https://www.ncbi.nlm.nih.gov/pubmed/30005145.

15. Weiss, Kurt R., Fabian F. Voigt, Douglas P. Shepherd, and Jan Huisken. "Tutorial: practical considerations for tissue clearing and imaging." *Nature protocols* 16, no. 6 (2021): 2732-2748. https://doi.org/10.1038/s41596-021-00502-8. https://pubmed.ncbi.nlm.nih.gov/34021294/.

16. Mai, H., J. Luo, L. Hoeher, R. Al-Maskari, I. Horvath, Y. Chen, F. Kofler, M. Piraud, J. C. Paetzold, J. Modamio, M. Todorov, M. Elsner, F. Hellal, and A. Ertürk. 2024. "Whole-body cellular mapping in mouse using standard IgG antibodies." *Nat Biotechnol* 42 (4): 617-627. https://www.nature.com/articles/s41587-023-01846-0. https://www.ncbi.nlm.nih.gov/pubmed/37430076.

17. Mai, H., Z. Rong, S. Zhao, R. Cai, H. Steinke, I. Bechmann, and A. Ertürk. 2022. "Scalable tissue labeling and clearing of intact human organs." *Nat Protoc* 17 (10): 2188-2215. https://doi.org/10.1038/s41596-022-00712-8. https://www.ncbi.nlm.nih.gov/pubmed/35859136.

18. Zhao, S., M. I. Todorov, R. Cai, R. A. -Maskari, H. Steinke, E. Kemter, H. Mai, Z. Rong, M. Warmer, K. Stanic, O. Schoppe, J. C. Paetzold, B. Gesierich, M. N. Wong, T. B. Huber, M. Duering, O. T. Bruns, B. Menze, J. Lipfert, V. G. Puelles, E. Wolf, I. Bechmann, and A. Ertürk. 2020. "Cellular and Molecular Probing of Intact Human Organs." *Cell* 180 (4): 796-812.e19. https://doi.org/10.1016/j.cell.2020.01.030. https://www.ncbi.nlm.nih.gov/pubmed/32059778.

19. Cai, R., C. Pan, A. Ghasemigharagoz, M. I. Todorov, B. Förstera, S. Zhao, H. S. Bhatia, A. Parra-Damas, L. Mrowka, D. Theodorou, M. Rempfler, A. L. R. Xavier, B. T. Kress, C. Benakis, H. Steinke, S. Liebscher, I. Bechmann, A. Liesz, B. Menze, M. Kerschensteiner, M. Nedergaard, and A. Ertürk. 2019. "Panoptic imaging of transparent mice reveals whole-body neuronal projections and skull-meninges connections." *Nat Neurosci* 22 (2): 317-327. https://doi.org/10.1038/s41593-018-0301-3. https://www.ncbi.nlm.nih.gov/pubmed/30598527.

20. Cai, R., Z. I. Kolabas, C. Pan, H. Mai, S. Zhao, D. Kaltenecker, F. F. Voigt, M. Molbay, T. L. Ohn, C. Vincke, M. I. Todorov, F. Helmchen, J. A. Van Ginderachter, and A. Ertürk. 2023. "Whole-mouse clearing and imaging at the cellular level with vDISCO." *Nat Protoc* 18 (4): 1197-1242. https://doi.org/10.1038/s41596-022-00788-2. https://www.ncbi.nlm.nih.gov/pubmed/36697871.

21. Qi, Y., T. Yu, J. Xu, P. Wan, Y. Ma, J. Zhu, Y. Li, H. Gong, Q. Luo, and D. Zhu. 2019. "FDISCO: Advanced solvent-based clearing method for imaging whole organs." *Sci Adv* 5 (1): eaau8355. https://doi.org/10.1126/sciadv.aau8355. https://www.ncbi.nlm.nih.gov/pubmed/30746463.

22. Merz, S. F., S. Korste, L. Bornemann, L. Michel, P. Stock, A. Squire, C. Soun, D. R. Engel, J. Detzer, H. Lörchner, D. M. Hermann, M. Kamler, J. Klode, U. B. Hendgen-Cotta, T. Rassaf, M. Gunzer, and M. Totzeck. 2019. "Contemporaneous 3D characterization of acute and chronic myocardial I/R injury and response." *Nat Commun* 10 (1): 2312. https://doi.org/10.1038/s41467-019-10338-2. https://www.ncbi.nlm.nih.gov/pubmed/31127113.

23. Henning, Y., C. Osadnik, and E. P. Malkemper. 2019. "EyeCi: Optical clearing and imaging of immunolabeled mouse eyes using light-sheet fluorescence microscopy." *Exp Eye Res* 180: 137-145. https://doi.org/10.1016/j.exer.2018.12.001. https://www.ncbi.nlm.nih.gov/pubmed/30578790.

24. Jing, D., S. Zhang, W. Luo, X. Gao, Y. Men, C. Ma, X. Liu, Y. Yi, A. Bugde, B. O. Zhou, Z. Zhao, Q. Yuan, J. Q. Feng, L. Gao, W. P. Ge, and H. Zhao. 2018. "Tissue clearing of both hard and soft tissue organs with the PEGASOS method." *Cell Res* 28 (8): 803-818. https://doi.org/10.1038/s41422-018-0049-z. https://www.ncbi.nlm.nih.gov/pubmed/29844583.

25. Klingberg, A., A. Hasenberg, I. Ludwig-Portugall, A. Medyukhina, L. Männ, A. Brenzel, D. R. Engel, M. T. Figge, C. Kurts, and M. Gunzer. 2017. "Fully Automated Evaluation of Total Glomerular Number and Capillary Tuft Size in Nephritic Kidneys Using Lightsheet Microscopy." *J Am Soc Nephrol* 28 (2): 452-459.https://doi.org/10.1681/ASN.2016020232. https://www.ncbi.nlm.nih.gov/pubmed/27487796.

26. Renier, N., E. L. Adams, C. Kirst, Z. Wu, R. Azevedo, J. Kohl, A. E. Autry, L. Kadiri, K. Umadevi Venkataraju, Y. Zhou, V. X. Wang, C. Y. Tang, O. Olsen, C. Dulac, P. Osten, and M. Tessier-Lavigne. 2016. "Mapping of Brain Activity by Automated Volume Analysis of Immediate Early Genes." *Cell* 165 (7): 1789-1802. https://doi.org/10.1016/j.cell.2016.05.007. https://www.ncbi.nlm.nih.gov/pubmed/27238021.

27. Renier, N., Z. Wu, D. J. Simon, J. Yang, P. Ariel, and M. Tessier-Lavigne. 2014. "iDISCO: a simple, rapid method to immunolabel large tissue samples for volume imaging." *Cell* 159 (4): 896-910. https://doi.org/10.1016/j.cell.2014.10.010. https://www.ncbi.nlm.nih.gov/pubmed/25417164.

28. Ertürk, A., K. Becker, N. Jährling, C. P. Mauch, C. D. Hojer, J. G. Egen, F. Hellal, F. Bradke, M. Sheng, and H. U. Dodt. 2012. "Three-dimensional imaging of solvent-cleared organs using 3DISCO." *Nat Protoc* 7 (11): 1983-95. https://doi.org/10.1038/nprot.2012.119. https://www.ncbi.nlm.nih.gov/pubmed/23060243.

29. Becker, K., N. Jährling, S. Saghafi, R. Weiler, and H. U. Dodt. 2012. "Chemical clearing and dehydration of GFP expressing mouse brains." *PLoS One* 7 (3): e33916. https://doi.org/10.1371/journal.pone.0033916. https://www.ncbi.nlm.nih.gov/pubmed/22479475.

30. Kosmidis, S., A. Negrean, A. Dranovsky, A. Losonczy, and E. R. Kandel. 2021. "A fast, aqueous, reversible three-day tissue clearing method for adult and embryonic mouse brain and whole body." *Cell Rep Methods* 1 (7): 100090. https://doi.org/10.1016/j.crmeth.2021.100090. https://www.ncbi.nlm.nih.gov/pubmed/34966901.

31. Pende, M., K. Vadiwala, H. Schmidbaur, A. W. Stockinger, P. Murawala, S. Saghafi, M. P. S. Dekens, K. Becker, R. Revilla-l-Domingo, S. C. Papadopoulos, M. Zurl, P. Pasierbek, O. Simakov, E. M. Tanaka, F. Raible, and H. U. Dodt. 2020. "A versatile depigmentation, clearing, and labeling method for exploring nervous system diversity." *Sci Adv* 6 (22): eaba0365. https://doi.org/10.1126/sciadv.aba0365. https://www.ncbi.nlm.nih.gov/pubmed/32523996.

32. Zhu, J., T. Yu, Y. Li, J. Xu, Y. Qi, Y. Yao, Y. Ma, P. Wan, Z. Chen, X. Li, H. Gong, Q. Luo, and D. Zhu. 2020. "MACS: Rapid Aqueous Clearing System for 3D Mapping of Intact Organs." *Adv Sci (Weinh)* 7 (8): 1903185. https://doi.org/10.1002/advs.201903185. https://www.ncbi.nlm.nih.gov/pubmed/32328422.

33. Lai, H. M., A. K. L. Liu, H. H. M. Ng, M. H. Goldfinger, T. W. Chau, J. DeFelice, B. S. Tilley, W. M. Wong, W. Wu, and S. M. Gentleman. 2018. "Next generation histology methods for three-dimensional imaging of fresh and archival human brain tissues." *Nat Commun* 9 (1): 1066. https://doi.org/10.1038/s41467-018-03359-w. https://www.ncbi.nlm.nih.gov/pubmed/29540691.

34. Yu, T., J. Zhu, Y. Li, Y. Ma, J. Wang, X. Cheng, S. Jin, Q. Sun, X. Li, H. Gong, Q. Luo, F. Xu, S. Zhao, and D. Zhu. 2018. "RTF: a rapid and versatile tissue optical clearing method." *Sci Rep* 8 (1): 1964. https://doi.org/10.1038/s41598-018-20306-3. https://www.ncbi.nlm.nih.gov/pubmed/29386656.

35. Li, W., R. N. Germain, and M. Y. Gerner. 2017. "Multiplex, quantitative cellular analysis in large tissue volumes with clearing-enhanced 3D microscopy (Ce3D)." *Proc Natl Acad Sci U S A* 114 (35): E7321-E7330. https://doi.org/10.1073/pnas.1708981114. https://www.ncbi.nlm.nih.gov/pubmed/28808033.

36. Hou, B., D. Zhang, S. Zhao, M. Wei, Z. Yang, S. Wang, J. Wang, X. Zhang, B. Liu, L. Fan, Y. Li, Z. Qiu, C. Zhang, and T. Jiang. 2015. "Scalable and DiI-compatible optical clearance of the mammalian brain." *Front Neuroanat* 9: 19. https://doi.org/10.3389/fnana.2015.00019. https://www.ncbi.nlm.nih.gov/pubmed/25759641.

37. Kurihara, D., Y. Mizuta, Y. Sato, and T. Higashiyama. 2015. "ClearSee: a rapid optical clearing reagent for whole-plant fluorescence imaging." *Development* 142 (23): 4168-79. https://doi.org/10.1242/dev.127613. https://www.ncbi.nlm.nih.gov/pubmed/26493404.

38. Susaki, E. A., K. Tainaka, D. Perrin, F. Kishino, T. Tawara, T. M. Watanabe, C. Yokoyama, H. Onoe, M. Eguchi, S. Yamaguchi, T. Abe, H. Kiyonari, Y. Shimizu, A. Miyawaki, H. Yokota, and H. R. Ueda. 2014. "Whole-brain imaging with single-cell resolution using chemical cocktails and computational analysis." *Cell* 157 (3): 726-39. https://doi.org/10.1016/j.cell.2014.03.042. https://www.ncbi.nlm.nih.gov/pubmed/24746791.

39. Susaki, E. A., K. Tainaka, D. Perrin, H. Yukinaga, A. Kuno, and H. R. Ueda. 2015. "Advanced CUBIC protocols for whole-brain and whole-body clearing and imaging." *Nat Protoc* 10 (11): 1709-27. https://doi.org/10.1038/nprot.2015.085. https://www.ncbi.nlm.nih.gov/pubmed/26448360.

40. Ke, M. T., S. Fujimoto, and T. Imai. 2013. "SeeDB: a simple and morphology-preserving optical clearing agent for neuronal circuit reconstruction." *Nat Neurosci* 16 (8): 1154-61. https://doi.org/10.1038/nn.3447. https://www.ncbi.nlm.nih.gov/pubmed/23792946.

41. Kuwajima, T., A. A. Sitko, P. Bhansali, C. Jurgens, W. Guido, and C. Mason. 2013. "ClearT: a detergent- and solvent-free clearing method for neuronal and non-neuronal tissue." *Development* 140 (6): 1364-8. https://doi.org/10.1242/dev.091844. https://www.ncbi.nlm.nih.gov/pubmed/23444362.

42. Hama, H., H. Kurokawa, H. Kawano, R. Ando, T. Shimogori, H. Noda, K. Fukami, A. Sakaue-Sawano, and A. Miyawaki. 2011. "Scale: a chemical approach for fluorescence imaging and reconstruction of transparent mouse brain." *Nat Neurosci* 14 (11): 1481-8. https://doi.org/10.1038/nn.2928. https://www.ncbi.nlm.nih.gov/pubmed/21878933.

43. Hama, H., Hiroyuki H., Kana N., Tetsushi H., Hiroshi K., Fumiyoshi I., Takeshi K., Takumi, A., Takashi, S., and Atsushi M. 2015. "ScaleS: An Optical Clearing Palette for Biological Imaging." *Nat Neuroscience* 18 (10): 1518–29. https://doi.org/10.1038/nn.4107. https://pubmed.ncbi.nlm.nih.gov/26368944/.

44. Yun, Dae Hee, Young-Gyun Park, Jae Hun Cho, Lee Kamentsky, Nicholas B. Evans, Alex Albanese, Katherine Xie, Justin Swaney, Chang Ho Sohn, Yuxuan Tian, Qiangge Zhang, Gabi Drummond, Webster Guan, Nicholas DiNapoli, Heejin Choi, Hae-Yoon Jung, Luzdary Ruelas, Guoping Feng, and Kwanghun Chung. 2019. "Ultrafast immunostaining of organ-scale tissues for scalable proteomic phenotyping." *bioRxiv*. https://doi.org/10.1101/660373

45. Park, Y. G., C. H. Sohn, R. Chen, M. McCue, D. H. Yun, G. T. Drummond, T. Ku, N. B. Evans, H. C. Oak, W. Trieu, H. Choi, X. Jin, V. Lilascharoen, J. Wang, M. C. Truttmann, H. W. Qi, H. L. Ploegh, T. R. Golub, S. C. Chen, M. P. Frosch, H. J. Kulik, B. K. Lim, and K. Chung. 2018. "Protection of tissue physicochemical properties using polyfunctional crosslinkers." *Nat Biotechnol*. https://doi.org/10.1038/nbt.4281. https://www.ncbi.nlm.nih.gov/pubmed/30556815.

46. Lee, E., J. Choi, Y. Jo, J. Y. Kim, Y. J. Jang, H. M. Lee, S. Y. Kim, H. J. Lee, K. Cho, N. Jung, E. M. Hur, S. J. Jeong, C. Moon, Y. Choe, I. J. Rhyu, H. Kim, and W. Sun. 2016. "ACT-PRESTO: Rapid and consistent tissue clearing and labeling method for 3-dimensional (3D) imaging." *Sci Rep* 6: 18631. https://doi.org/10.1038/srep18631. https://www.ncbi.nlm.nih.gov/pubmed/26750588.

47. Murray, E., J. H. Cho, D. Goodwin, T. Ku, J. Swaney, S. Y. Kim, H. Choi, Y. G. Park, J. Y. Park, A. Hubbert, M. McCue, S. Vassallo, N. Bakh, M. P. Frosch, V. J. Wedeen, H. S. Seung, and K. Chung. 2015. "Simple, Scalable Proteomic Imaging for High-Dimensional Profiling of Intact Systems." *Cell* 163 (6): 1500-14. https://doi.org/10.1016/j.cell.2015.11.025. https://www.ncbi.nlm.nih.gov/pubmed/26638076.

48. Yang, B., J. B. Treweek, R. P. Kulkarni, B. E. Deverman, C. K. Chen, E. Lubeck, S. Shah, L. Cai, and V. Gradinaru. 2014. "Single-cell phenotyping within transparent intact tissue through whole-body clearing." *Cell* 158 (4): 945-958. https://doi.org/10.1016/j.cell.2014.07.017. https://www.ncbi.nlm.nih.gov/pubmed/25088144.

49. Klimas, A., B. R. Gallagher, P. Wijesekara, S. Fekir, E. F. DiBernardo, Z. Cheng, D. B. Stolz, F. Cambi, S. C. Watkins, S. L. Brody, A. Horani, A. L. Barth, C. I. Moore, X. Ren, and Y. Zhao. 2023. "Magnify is a universal molecular anchoring strategy for expansion microscopy." *Nat Biotechnol* 41 (6): 858-869. https://doi.org/10.1038/s41587-022-01546-1. https://www.ncbi.nlm.nih.gov/pubmed/36593399.

50. Truckenbrodt, S., M. Maidorn, D. Crzan, H. Wildhagen, S. Kabatas, and S. O. Rizzoli. 2018. "X10 expansion microscopy enables 25-nm resolution on conventional microscopes." *EMBO Rep* 19 (9). https://doi.org/10.15252/embr.201845836. https://www.ncbi.nlm.nih.gov/pubmed/29987134.

51. Chang, J. B., F. Chen, Y. G. Yoon, E. E. Jung, H. Babcock, J. S. Kang, S. Asano, H. J. Suk, N. Pak, P. W. Tillberg, A. T. Wassie, D. Cai, and E. S. Boyden. 2017. "Iterative expansion microscopy." *Nat Methods* 14 (6): 593-599. https://doi.org/10.1038/nmeth.4261. https://www.ncbi.nlm.nih.gov/pubmed/28417997.

52. Tillberg, P. W., F. Chen, K. D. Piatkevich, Y. Zhao, C. C. Yu, B. P. English, L. Gao, A. Martorell, H. J. Suk, F. Yoshida, E. M. DeGennaro, D. H. Roossien, G. Gong, U. Seneviratne, S. R. Tannenbaum, R. Desimone, D. Cai, and E. S. Boyden. 2016. "Protein-retention expansion microscopy of cells and tissues labeled using standard fluorescent proteins and antibodies." *Nat Biotechnol* 34 (9): 987-92. https://doi.org/10.1038/nbt.3625. https://www.ncbi.nlm.nih.gov/pubmed/27376584.

Authors

Dr. Jan Frankowski, Applications Scientist, Bruker
Dr. Jürgen Mayer, Senior Product and Applications Specialist, Bruker
Dr. Elisabeth Kugler, External Marcom Specialist
Melissa Martin, Life Science Writer, Bruker

Further Resources

www.bruker.com/light-sheet

Bruker Fluorescence Metrology

Heidelberg • Germany

productinfo@bruker.com

Light-Sheet Fluorescence Microscopy | See Biology Across All Scales

www.bruker.com/tissue-clearing